On the influence of ionization-recombination and radiative losses in thermal plasma modelling

ON THE INFLUENCE OF IONIZATION-RECOMBINATION AND RADIATIVE LOSSES IN THERMAL PLASMA MODELLING

D.A. BENOY, J.A.M. van der MULLEN and D.C. SCHRAM,
Department of Physics, Eindhoven University of Technology,
P.O. Box 513, 5600 MB Eindhoven, The Netherlands.

ABSTRACT. We have investigated the influences of the ionization/recombination and the radiative energy loss on the particle and temperature distributions in a pure argon inductively coupled plasma. To calculate the flow and the temperature field an axi-symmetric 2-temperature numerical fluid model has been used. Comparisons were made between results obtained by using different types of data for the effective ionization/recombination coefficient and for the radiative energy losses. Experimental data and a hybrid collisional-radiative model were used for the effective ionization and recombination coefficient. For the total radiative loss also experimental data and a non-local thermal equilibrium model were applied. With the numerical fluid model it was possible to trace the effects of non-equilibrium aspects of ionization and recombination on the electron and heavy particle temperature and the electron density profiles. The electron density is the most suitable parameter to distinguish the different sets for the ionization/recombination coefficient and the radiative energy loss.

1 Introduction

The use of thermal argon plasmas can be found in various number of applications. Inductively coupled plasmas (ICP) and expanding cascaded arcs are well-known in the field of spectrochemical analysis and carbon/silicon deposition, respectively. For the theoretical investigation of thermal plasmas, models have been developed in order to study the various physical processes and their interrelationships. An obvious advantage in using models is that the effect of different operating conditions can be investigated, which is important with respect to the optimization of the various applications. For an adequate characterisation of these plasmas we rely on a non-equilibrium description of the plasma. Both the electron temperature and heavy particle temperature are required in order to understand the elementary balances and the transport phenomena. This implies that the knowledge is required of the effective volumetric ionization/recombination coefficient and radiative energy losses. In this study the influence of different non-equilibrium models for the ionization/recombination and radiative losses on the temperature and the particle density in the plasma, is investigated. The calculations are applied to an ICP configuration.

2 Model

To calculate the flow, particle density and temperature distribution in the plasma a numerical fluid model is used in which the plasma is considered to be laminar, stationary, two-dimensional axisymmetric and quasi-neutral. To account for non local thermal equilibrium (LTE) effects a two-temperature approach is adopted in which the plasma is considered as being composed of electrons and heavy particles. A two-dimensional self-consistent vectorpotentialmodel is used to calculate the electromagnetic field. [1] With this model large excitation frequencies for which the plasma skindepth is smaller than the plasmaradius can also be handled. As a result a large RF-frequency domain (1−100MHz) can be covered. [1, 2]
With the aforementioned assumptions the transport equations which describes the plasma flow are

$$\vec{\nabla}\cdot(\rho\vec{v}) = 0 \tag{1}$$

$$\vec{\nabla}\cdot(n_e\vec{v}) - \vec{\nabla}\cdot(D_A\vec{\nabla}n_e) = n_e n_a S_{CR} - n_e n_+ \alpha_{CR} \tag{2}$$

$$\vec{\nabla}\cdot(\rho\vec{v}\,\vec{v}) = -\vec{\nabla}p - \vec{\nabla}\cdot\boldsymbol{\Pi} + \vec{J}\times\vec{B} \tag{3}$$

$$\vec{\nabla}\cdot[(\frac{5}{2}n_e kT_e + E^+)\vec{v}] - \vec{\nabla}\cdot(\kappa_e\vec{\nabla}T_e) = \vec{J}\cdot\vec{E} - Q_{eh} - Q_{rad} \tag{4}$$

$$\vec{\nabla}\cdot[(\frac{5}{2}(n_e+n_a)kT_h)\vec{v}] - \vec{\nabla}\cdot(\kappa_h\vec{\nabla}T_h) = \vec{v}\cdot\vec{\nabla}p + Q_{eh} \tag{5}$$

where the symbols are explained in the Nomenclature. The ionization and recombination coefficients S_{CR} and α_{CR}, respectively, reflect the coupling between the microscopic and macroscopic balance equations. For the effective ionization and recombination coefficient experimental data of DESAI and CORCORAN[3] and a collisional radiative model with a hybrid cut-off technique have been used. [4] For the total radiative energy losses different data have been used, one experimental data set of Ref. 5 and two theoretical data sets WILBERS et al[6] and BENOY et al[7]. The radiative energy losses according to Ref. 6 account for non-equilibrium in the sense that only the neutral groundstate may deviate from its Saha population. In the work of Ref. 7 the degree of non-equilibrium has been extended by allowing that the atomic state distribution function may deviate from the Saha equation. The total radiative loss is then a function of n_e, T_e and the ionization degree. In both theoretical data sets for the radiative energy loss it is assumed that the plasma is optically thin except for the resonance transitions for which the plasma is optically thick.

The system of equations (1 − 5) as well as the vectorpotential equation is solved by the control volume method based on the SIMPLE algorithm of PATANKAR.[8] A modified implementation of SIMPLE as described by RHIE is used. [9]

3 Computational results

Model calculations are applied to a 3MHz generated ICP. The plasma configuration is shown Fig. 1, the specification of the torch dimensions and the operating conditions are given in Table 1. The coil has 3 windings.

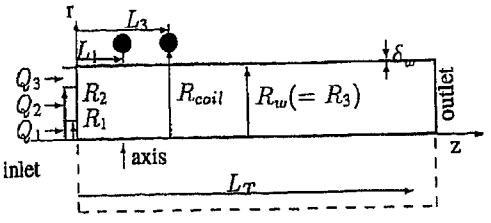

Figure 1. The ICP torch geometry. The computational domain is enclosed by thick lines.

R_1	0.0017 m	f	3MHz
R_2	0.0188 m	P_0	5kW
R_3	0.0250 m	Q_1	1 ℓ/m
R_{coil}	0.0330 m	Q_2	3 ℓ/m
L_T	0.170 m	Q_3	21 ℓ/m
L_1	0.030 m	L_2	0.060 m
L_3	0.090 m	p	1 atm.

Table 1. Torch specification of the 3MHz ICP.

The following model calculations were carried out:

1. S_{CR} and α_{CR}: DESAI and CORCORAN. [3]
   Radiation loss: EVANS and TANKIN (DC-ET). [5]

2. S_{CR} and α_{CR}: DESAI and CORCORAN. [3]
   Radiation loss: WILBERS et al (DC-W). [6]

3. S_{CR} and α_{CR}: DESAI and CORCORAN. [3]
   Radiation loss: BENOY et al (DC-B). [7]

4. S_{CR} and α_{CR}: BENOY et al. [4]
   Radiation loss: BENOY et al (B-B).[7]

Run	T_e(max) (K)	r^{max} $\times 10^{-3}$m	z^{max} $\times 10^{-3}$m	$\int Q_{rad} dV$ (W)
1: DC-ET	9720	15.3	87.7	650
2: DC-W	9140	16.6	87.7	950
3: DC-B	9860	13.1	93.0	610
4: B-B	10650	13.1	87.7	715
Run	n_e(max) (m^{-3})			
1: DC-ET	1.13×10^{22}	14.2	93.0	
2: DC-W	5.90×10^{21}	16.6	87.7	
3: DC-B	1.30×10^{22}	13.1	93.0	
4: B-B	1.71×10^{22}	9.7	93.0	

Table 2: Maximum values for the T_e and n_e profiles and the total radiative loss for the different runs.

In Table 2 the values and the positions maxima of the T_e and n_e profiles are shown for the different runs. Radial distributions of n_e and T_e for run1 at z=0.03, 0.09 and 0.15m are shown in Fig. 2. The first two axial positions correspond with the first and last winding of the coil. At the first winding position both n_e and T_e do not show an off-axis maximum. Diffusion for electrons and conduction for the temperature and recirculation near the torch inlet are responsible for the fact that the profile has its maximum on the axis. In Ref. 1 it can be seen that this recirculation is

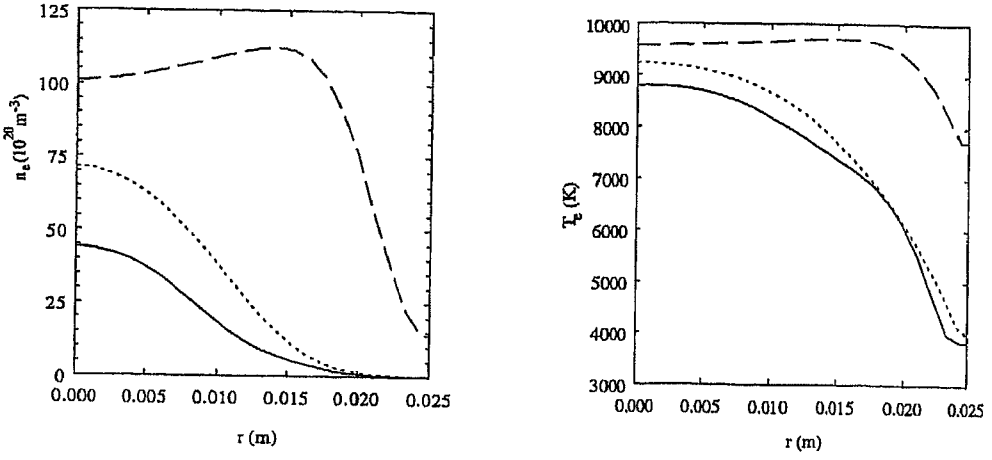

Figure 2: Radial n_e and T_e profiles calculated with run DC-ET for various axial positions (z=0.03 (full line), 0.09 (broken line), 0.15m (dotted line)).

accompanied with a back flow near the axis of about 5m/sec. Using this value we can compare the axial convection component $|\vec{\nabla} \cdot (n_e \vec{v})| \sim |5 \times 10^{21} \times (-5)/10^{-2}|$ with the radial diffusion component $|\vec{\nabla} \cdot (D_A \vec{\nabla} n_e)| \sim |5 \times 10^{21}(2 \times 10^{-3})/(5 \times 10^{-3})^2|$. It turns out that recirculation is the main transport mechanism for heating the central region near the torch inlet. Radial and axial distributions of T_e and radial distributions of T_h and n_e are shown in Figs. 3 and 4, respectively. The radial distributions are shown for z=0.087m corresponding with the last winding of the coil and for which the maximum values are found. In the following the nomenclature "inner region" is used to denote the region $r < r^{max}$ where r^{max} is the radial position of the profile maximum. Comparison of the radial distribution of T_e and T_h of the same runs reveals that $T_e \approx T_h$ in the inner region. This is due to the high collision frequency between electrons and heavy particles. For the outer regions the differences between T_e and T_h increase towards the torch wall. Due to these colder regions the energy transfer from electron to heavy particles decreases.

Influence of radiative losses. By comparing the results of runs 1 – 3 the influence of the radiative loss on the calculated profiles is investigated. A comparative study of the influence of the radiative loss is also performed by PROULX et al[10] in which radiative loss data of CRAM were compared with data of Refs. 5 and 11. In Table 2 the volumetric radiative losses are also shown. The integration is performed over the whole computational domain. The computational data of WILBERS et al[6] based on a non-LTE model allowing T_e and n_e to be decoupled, give the highest total radiative loss. The non-LTE model of BENOY et al[7] for the radiative loss, leads to a total radiative loss differing 6% with the calculations based on the experimental data of EVANS and TANKIN. [5] This apparent agreement between the run DC-ET and DC-B merely is a coincidence. The radiative loss data of Ref. 5 fitted by MILLER and AYEN[12] have a temperature threshold at 9500 K and below this threshold the radiative loss is zero. Above this value the radiative loss increases more than the radiation loss predicted by BENOY et al. [7] The radiative loss (Q_{rad}) of Ref. 7 does not show a temperature threshold. The difference in radiation loss above 9500 K between the two sets of data of Refs. 7 and 12 is compensated by the radiative loss in the lower temperature region in the data set of Ref. 7.

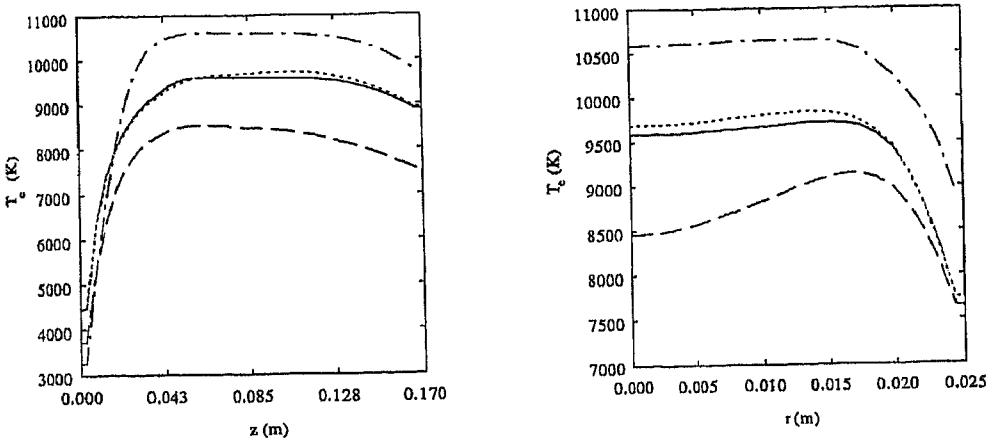

Figure 3: Influence of the different models for ionization/recombination and radiation on the axial (r=0) and the radial (z=0.087m) electron temperature profiles. (—): run DC-ET, (– – –): run DC-W, - - -: run DC-B, (– · –): run B-B.

It should be stressed that the radiative loss data of Refs. 6 and 7 are based on the assumption that the free-bound to the ground state may be neglected. This is a reasonable assumption since the free path of a resonant recombination photon $\lambda_f = 1/n_a\sigma_{ph}$, where the ground state photo-ionization cross-section $\sigma_{ph} \sim 3.5 \times 10^{-21}\text{m}^2$ and $n_a \sim 10^{24}\text{m}^{-3}$, is about 0.003m which is smaller than the plasma dimension. [13]

A larger radiation loss results in an overall lower temperature (electron and heavy particle) and n_e field. The differences between the maximum T_e are 700 $\sim$ 1400K while the maximum values for n_e differ with a factor of 2. On the axis the differences can be as high as 1000K (Fig. 3) while the differences in n_e increase up to a factor of 4 (Fig. 4). The n_e is much more sensitive for radiation losses than T_e. With accurate measurements of n_e it is possible to distinguish between the different sets for the radiative loss data. We can conclude that n_e is a more suitable parameter in tracing non-equilibrium processes than T_e. [14]

Influence of ionization/recombination. In this part we consider the consequences of the differences between the formulae for ionization/recombination of DESAI and CORCORAN[3] and BENOY et al[4]. Comparing the temperature and electron density distributions calculated with the different runs we see that in the hottest part where $T_e \approx T_h$ the temperature and n_e differ 1000 K and a factor 1.4, respectively. The reason for this difference is found in the expression of the effective ionization coefficient S_{CR}^{DC} using the data of DESAI and CORCORAN. From the expression for the recombination coefficient given by Ref. 3, we find

$$S_{CR}^{DC} = 2.56 \times 10^{25-(3410/T_e)} T_e^{-0.3} n_e^{-1.64} \exp\left(\frac{-E^+}{kT_e}\right), \text{m}^3/\text{sec} \qquad (6)$$

in which T_e is expressed in K. A remarkable feature of this expression is the negative power of n_e. The background is that S_{CR}^{DC} is based on dissociative recombination. Dissociative recombination of Ar_2^+ is effective if the resulting excited atom makes a radiative transition and is not reionized. In order that radiative decay takes place n_e may not be too high otherwise excitation or ionization of

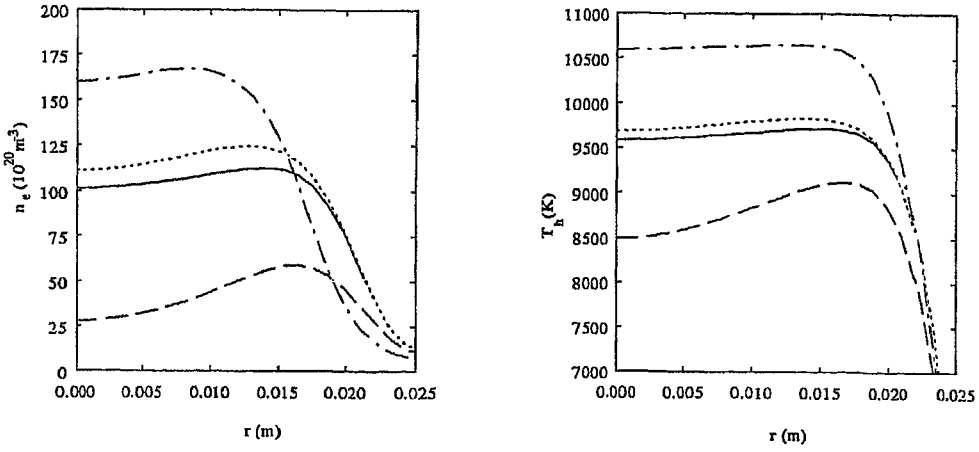

Figure 4: Radial distribution of n_e (left) and T_h (right) for z=0.087m. (—): run DC-ET, (– – –): run DC-W, - - -: run DC-B, (– · –): run B-B.

this level would occur. These arguments make it plausible that dissociative recombination scales with a negative power of n_e.

Ionization leads to an increase of n_e so that according to Eq. (6) S_{CR}^{DC} will decrease by the increase of n_e if T_e would not change. In contrast, the S_{CR} based on the collisional-radiative model of Ref. 4 does not show this n_e dependency. Hence, by using S_{CR}^{DC} less electrons are created then when S_{CR} of Ref. 4 is used.

4 Conclusion

The results presented in this work demonstrate the usefulness of model calculations in tracing the effects of non-equilibrium aspects of ionization/recombination and radiation losses on the temperature and electron density profiles in thermal plasmas. In all cases the electron density is a suitable parameter to distinguish between the different models for the aforementioned processes. Accurate measurements of the electron density in this type of plasmas can give a decisive answer to the question of which model is the best in describing ionization/recombination and radiative energy losses.

References

[1] J. Mostaghimi and M.I. Boulos, *Plasma Chem. Plasma Proc.*, **9**(1), 25, (1989).

[2] F.H.A.G. Fey, W.W. Stoffels, J.A.M. van der Mullen, B. van der Sijde and D.C. Schram, *Spectrochim. Acta*, **46B**, 885, (1991).

[3] S.V. Desai and W.H. Corcoran, *J. Quant. Spectrosc. Radiat. Transfer*, **9**, 1371, (1969).

[4] D.A. Benoy, J.A.M. van der Mullen, and D.C. Schram, *J. Quant. Spectrosc. Radiat. Transfer*, **46**, 195, 1991.

[5] D.L. Evans and R.S. Tankin, *Phys. of Fluids*, **10**, 1137, (1967).

[6] A.T.M. Wilbers, J.J. Beulens, and D.C. Schram, *J. Quant. Spectrosc. Radiat. Transfer*, **46**(5), 385, (1991).

[7] D.A. Benoy, J.A.M. van der Mullen, and D.C. Schram, *J. Phys. D: Appl. Phys.* **26**, 1408, (1993).

[8] S.V. Patankar, *Numerical Heat Transfer and Fluid Flow*, McGraw-Hill, New York, (1980).

[9] C.M. Rhie and W.L. Chow, *AIAA J.* **27**, 1167, (1983).

[10] P. Proulx, J. Mostaghimi, and M.I. Boulos, *Int J. Heat. Mass Transfer*, **34(10)**, 2571, (1991).

[11] A. Mensing and L. Boedeker, *Theoretical Investigations of RF Induction Heated Plasmas*, NASA CR-1312, 61, (1969).

[12] R.C. Miller and R.J. Ayen, *J. Appl. Phys.*, **40**, 5260, (1969).

[13] G. Trommer, *Proc XV ICPIG, Minsk*, 1614, (1981).

[14] B. van der Sijde and J.A.M. van der Mullen, *J. Quant. Spectrosc. Radiat. Transfer*, **44**, 39, (1990).

Nomenclature

$\vec{B}$	magnetic induction	Q_{rad}	radiative energy losses
D_A	ambipolar diffusion coefficient	S_{CR}	ionization coefficicient
$\vec{E}$	electric field	T_e	electron temperature
E^+	ionization energy	T_h	heavy particle temperature
$\vec{J}$	electric current density	$\vec{v}$	plasma velocity
k	Boltzmann constant	α_{CR}	recombination coefficient
n_a	neutral particle density	κ_e	elec.therm. cond. coef.
n_e	electron density	κ_h	heavy part.therm.cond.coef.
n_+	ion density	ρ	density
p	pressure	Π	viscosity tensor
Q_{eh}	elec.-heavy part. energy transfer		